

Thermal decomposition of cobalt nitrate compounds: Preparation of anhydrous cobalt(II)nitrate and its characterisation by Infrared and Raman spectra

Claus Ehrhardt¹, Mimoza Gjikaj², Wolfgang Brockner*

Institute of Inorganic and Analytical Chemistry, Clausthal University of Technology, Paul-Ernst-Strasse 4, D-38678 Clausthal-Zellerfeld, Germany

Received 24 February 2005; received in revised form 12 April 2005; accepted 14 April 2005

Abstract

The thermal decomposition of $\text{Co}(\text{NO}_3)_2 \cdot 6\text{H}_2\text{O}$ (**1**) as well as that one of $\text{NO}[\text{Co}(\text{NO}_3)_3]$ ($\text{Co}(\text{NO}_3)_2 \cdot \text{N}_2\text{O}_4$) (**2**) was followed by thermogravimetric (TG) measurements, X-ray recording and Raman and IR spectra. The stepwise decomposition reactions of **1** and **2** leading to anhydrous cobalt(II)nitrate (**3**) were established. In N_2 atmosphere, cobalt oxides are finally formed whereas in H_2/N_2 (10% H_2) cobalt metal is produced. Rapid heating of cobalt(II)nitrate hexahydrate causes melting (formation of a hydrate melt) and therefore side reactions in the hydrate melt by incoupled reactions and evolution/evaporation of different species as, e.g., HNO_3 , NO_2 , etc. In case of larger amounts in dense packing in the sample container, the formation of oxo(hydroxo)nitrates is possible at higher temperature. For **2**, its thermal decomposition to **3** was followed and its decomposition mechanism is proposed.

© 2005 Elsevier B.V. All rights reserved.

Keywords: $\text{Co}(\text{NO}_3)_2$; $\text{Co}(\text{NO}_3)_2 \cdot 6\text{H}_2\text{O}$; $\text{NO}[\text{Co}(\text{NO}_3)_3]$; Thermochemistry; Raman and IR spectra

1. Introduction

Beside the fact that the knowledge of anhydrous transition metal nitrates is scanty such metal nitrates (hydrates) are widely used for preparation of high-surface area materials as, e.g., for catalysts as oxides and metals [1–3]. Especially, cobalt and alumina supported cobalt oxide catalysts have been widely applied in Fischer–Tropsch synthesis, hydrocracking and selective hydrogenation reactions [4–7]. The Fischer–Tropsch synthesis involves the conversion of carbon monoxide and hydrogen to predominantly hydrocarbon products, either olefins or paraffins. Therefore, the thermal decomposition processes of metal nitrate hydrates are important to know. Even in most recent corresponding publications

confusing and partially contradictory theories and facts are presented [8–15]. Especially thermogravimetry (TG) in its quasi-isothermal variant is a very helpful tool for the study of decomposition reactions in combination with structure sensitive methods as, e.g., Raman and IR spectroscopy and X-ray diffraction measurements.

In the course of studies on anhydrous metal nitrates [16] also $\text{NO}[\text{Co}(\text{NO}_3)_3]$ [17,18] was prepared and investigated thermogravimetrically.

2. Experimental

2.1. Substances and methods

Commercial $\text{Co}(\text{NO}_3)_2 \cdot 6\text{H}_2\text{O}$ (Merck, p.A.) was used as received. $\text{NO}[\text{Co}(\text{NO}_3)_3]$ was prepared out of CoCl_2 and N_2O_5 according to Ref. [18].

The thermal decomposition processes were pursued by thermogravimetric analysis (TG) using a thermobalance (Sar-

* Corresponding author. Tel.: +49 5323 722656; fax: +49 5323 722995.

E-mail addresses: claus.ehrhardt@tu-clausthal.de (C. Ehrhardt),

mimoza.gjikaj@tu-clausthal.de (M. Gjikaj),

wolfgang.brockner@tu-clausthal.de (W. Brockner).

¹ Tel.: +49 5323 722484; fax: +49 5323 722995.

² Tel.: +49 5323 722887; fax: +49 5323 722995.

torius, type 4201) in which the sample compartment is separated and kept magnetically in suspension (magnetic suspension balance). Therewith, it is possible to investigate decomposition reactions evolving corrosive gases as, e.g., HNO_3 , NO_x , etc., as well as using different atmospheres. By a home-made computer-supported driving, the heating rate is controlled/varied by relative mass loss in response to the sample decomposition allowing quasi-isothermal measurements, too [19]. Further details are given in Section 3. In effect, this method is comparable to the “Dynamic Rate Controlled Method” [20].

The FT-Raman spectra were recorded with a Raman module FRA 106 (Nd:YAG laser: 1064 nm, <200 mW) attached to a Bruker IFS 66v interferometer. Corresponding FT-IR spectra were obtained from KBr (sample) pellets (where the pellet is protected/isolated by an inert BaF_2 or a C_{60} layer) with the mentioned FT-IR interferometer. X-ray powder diffraction measurement was carried out with a STADI P (Fa. Stoe) at room temperature in a N_2 atmosphere and $\text{Cu K}\alpha$ radiation.

3. Results and discussion

3.1. Thermal decomposition of cobalt(II)nitrate hexahydrate (**1**)

The very slow thermal decomposition of **1**, presented in Fig. 1, reveals the stepwise formation of distinct hydrates as tetra- and di-hydrate, respectively, and of anhydrous cobalt(II)nitrate as a pink coloured product. To elucidate the unusual quasi-isothermal driving modus of the investigation method exemplarily the time dependence on the mass loss and on the temperature, respectively, is shown in Fig. 2. The used atmosphere (N_2 or H_2/N_2) has no influence for the dehy-

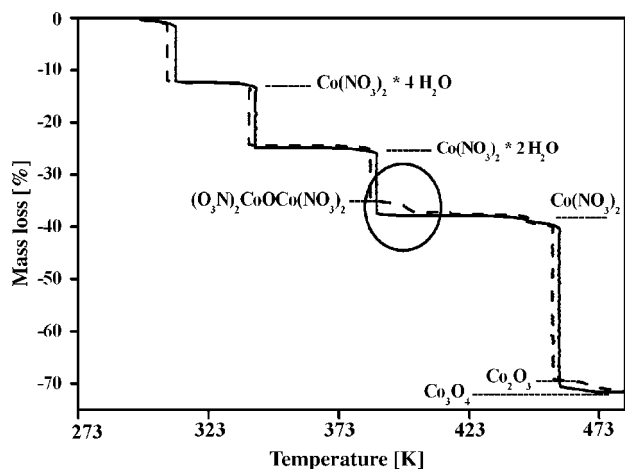


Fig. 1. Thermal decomposition (TG) of cobalt(II)nitrate hexahydrate in N_2 atmosphere showing the influence of sample loading and possible side reaction with leaving water (encirclement): (a) full line, 180 mg and (b) dotted/broken line, 291 mg. Temperature range, 293–773 K; heating rate between the quasi-isothermal decomposition steps, 0.6 K min^{-1} .

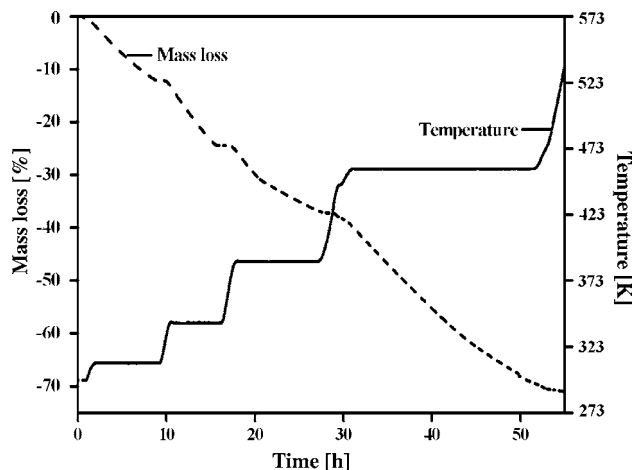


Fig. 2. Mass loss and temperature process during the thermal decomposition (TG) of **1** (for the TG curve of Fig. 1 elucidating the unusual (quasi-isothermal) driving modus).

dration steps. The further thermal decomposition of **3** results in the formation of the cobalt oxides Co_2O_3 and Co_3O_4 in N_2 atmosphere, whereas in H_2/N_2 finally metallic cobalt is generated (Figs. 1 and 3). All the corresponding experimental details and thermo-analytical characteristics including all corresponding chemical reactions are collected in Table 1 and indicated in Figs. 1 and 3, respectively.

Different sample loadings result in slightly differing degradation temperatures caused by an adjusted relative mass loss in the quasi-isothermal modus driving (cf. Fig. 1; Table 1). If partial reaction of the leaving water is possible in the third step (small sample container, greater sample amount, dense packing) cobalt(III)oxonitrate is formed likely according to the calculated mass loss and the proposed equation (Fig. 1,

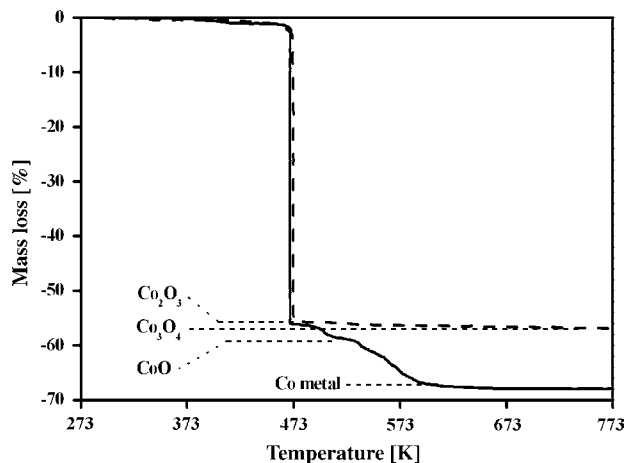


Fig. 3. Thermal decomposition (TG) of anhydrous $\text{Co}(\text{NO}_3)_2$ in N_2 and H_2/N_2 (10% H_2) atmosphere (full line), respectively, in the range 293–773 K. Heating rate between the quasi-isothermal decomposition steps, 0.6 K min^{-1} .

Table 1
Thermal decomposition reactions of **1** and **2**, and their characteristics (cf. Figs. 1–4)

Reaction/step	T (K) ^a	Δm (%) ^b		Atmosphere
		Experimental	Calculated	
(1) $\text{Co}(\text{NO}_3)_2 \cdot 6\text{H}_2\text{O} \rightarrow \text{Co}(\text{NO}_3)_2 \cdot 4\text{H}_2\text{O} + 2\text{H}_2\text{O}$	~308	12.3	12.38	N_2 ; H_2/N_2
(2) $\text{Co}(\text{NO}_3)_2 \cdot 4\text{H}_2\text{O} \rightarrow \text{Co}(\text{NO}_3)_2 \cdot 2\text{H}_2\text{O} + 2\text{H}_2\text{O}$	~340	24.8	24.75	N_2 ; H_2/N_2
(3) $\text{Co}(\text{NO}_3)_2 \cdot 2\text{H}_2\text{O} \rightarrow \text{Co}(\text{NO}_3)_2 + 2\text{H}_2\text{O}$	~383	37.5	37.12	N_2 ; H_2/N_2
(3a) Possible side reaction ^c , $2\text{Co}(\text{NO}_3)_2 \cdot 2\text{H}_2\text{O} \rightarrow [\text{Co}(\text{NO}_3)_2]_2\text{O} + \text{H}_2 + 3\text{H}_2\text{O}$	~385	34.7	34.37	N_2 ; H_2/N_2
(3b) $[\text{Co}(\text{NO}_3)_2]_2\text{O} \rightarrow 2\text{Co}(\text{NO}_3)_2 + 1/2\text{O}_2$	~398	37.5	37.12	N_2 ; H_2/N_2
(4a) $2\text{Co}(\text{NO}_3)_2 \rightarrow \text{Co}_2\text{O}_3 + \text{N}_2\text{O}_4 + \text{N}_2\text{O}_5$	~458 ^d	71.0	71.50	N_2 ; H_2/N_2
(4b) $3\text{Co}(\text{NO}_3)_2 \rightarrow \text{Co}_3\text{O}_4 + \text{N}_2\text{O}_4 + 2\text{N}_2\text{O}_5$		72.4	72.20	
(5a) $\text{Co}_2\text{O}_3 + 3\text{H}_2 \rightarrow 2\text{Co} + 3\text{H}_2\text{O}$	~458 ^d		Fig. 3	H_2/N_2
(5b) $\text{Co}_3\text{O}_4 + 4\text{H}_2 \rightarrow 3\text{Co} + 4\text{H}_2\text{O}$				
(6) $\text{NO}[\text{Co}(\text{NO}_3)_3] \rightarrow \text{Co}(\text{NO}_3)_2 + 2\text{NO}_2$	~343	33.5	33.46	N_2 (Fig. 4)

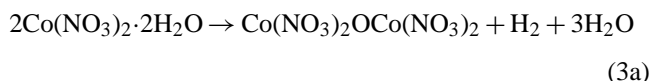
^a Decomposition temperature, slightly dependent on sample amount (cf. Section 3).

^b In relation to the starting compound **1**, and for Eq. (6) to **2**.

^c $(\text{NO}_3)_2\text{CoOC}(\text{NO}_3)_2$: cf. Section 3.

^d Beginning.

encirclement):



This oxonitrate is decomposed into **3** by further heating (Fig. 1; Table 1, Eq. (3b)).

Rapid heating of **1** causes a hydrate melt changing the system drastically by side reactions and evaporation of HNO_3 and other species. Such a corresponding TG curve (cf. Fig. 2 in Ref. [13]) is contourless and dependent on experimental conditions according to own measurements, too. The formation of a hydrate melt of **1** might be excluded by the storage of **1** over P_4O_{10} in a desiccator (1 week) yielding the tetrahydrate only.

The low temperature decomposition behaviour of Pb, Cu, Cd and Ag nitrates in vacuo was investigated by residual gas analysis [11,12]. Several metals containing species as MeO, $\text{Me}(\text{NO}_3)^+$ and Me_2^+ were detected in the gas phase. Only $\text{Pb}(\text{NO}_3)_2$ and $\text{Cd}(\text{NO}_3)_2$ are comparable to the here relevant $\text{Co}(\text{NO}_3)_2$ for which no such species are found (Table 1).

Recently, the thermal decomposition of molten AgNO_3 and $\text{Cd}(\text{NO}_3)_2$ was studied [21,22]. For $\text{Cd}(\text{NO}_3)_2$, which is comparable to $\text{Co}(\text{NO}_3)_2$, the evolution of oxygen (O atoms) was detected. This might be interpreted as an indication for the formation of nitrite, which is not found for $\text{Co}(\text{NO}_3)_2$.

3.2. Thermal decomposition of nitrosyl nitratocobaltate, $\text{NO}[\text{Co}(\text{NO}_3)_3]$

Anhydrous cobalt(II)nitrate is formed also by the thermal decomposition of **2** (Fig. 4; Table 1) under milder conditions. Both $\text{Co}(\text{NO}_3)_2$ products, obtained by thermal degradation of **1** and **2**, respectively, show identical properties proved by Raman and IR spectra as well as by X-ray diffraction pattern.

In Fig. 5, the X-ray diffraction pattern of **3** is given. Suited single crystals for crystal structure determination could not be obtained.

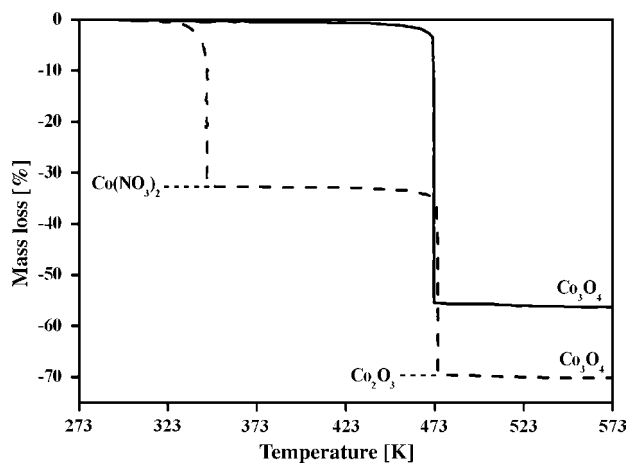


Fig. 4. Thermal decomposition (TG) of $\text{NO}[\text{Co}(\text{NO}_3)_3]$ in comparison to that of $\text{Co}(\text{NO}_3)_2$ in the range 293–573 K in N_2 atmosphere. Heating rate between the quasi-isothermal decomposition steps, 1.2 K min^{-1} . $\text{NO}[\text{Co}(\text{NO}_3)_3]$, full line; $\text{Co}(\text{NO}_3)_2$, dotted line.

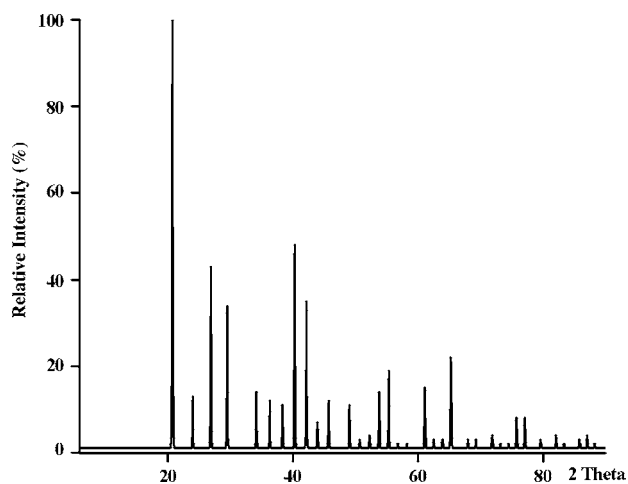


Fig. 5. X-ray powder diffraction pattern (Cu $\text{K}\alpha$ radiation) of $\text{Co}(\text{NO}_3)_2$.

Table 2
IR and Raman frequencies (cm^{-1}) of $\text{Co}(\text{NO}_3)_2$ (**3**) and $\text{Co}(\text{NO}_3)_2 \cdot 6\text{H}_2\text{O}$ along with their relative intensities and proposed assignments

$\text{Co}(\text{NO}_3)_2$		$\text{Co}(\text{NO}_3)_2 \cdot 6\text{H}_2\text{O}$		NO_3^- /solution [28]
Raman	IR	Raman	IR	D_{3h} /assignment
			3340 vbr	(H_2O)
	2772 vw			
	2760 vw			
	2428 vw		2427 vw	Combination bands
	2396 vw		2396 vw	
	1773 vw			
	1763 vw		1763 vw	
	(1632 vw, br)		1631 m, br	(H_2O)
			1461 w	(H_2O)
1446 w-m				
1392 vw	1389 vs		1384 vs	1390 (ν_{as}/E' ; IR, R)
	1356 vs		1355 vw	
1086 sh				
1079 vs		1057 vs		1057 (ν_{s}/A'_1 ; R)
	1050 vw			
	1032 w	1040 w	1033 m	
	829 s		829 m	830 (γ/A'_2 ; IR)
	806 m		807 w	
	797 vw, sh			
750 m-s	752 w		751 vw	720 (δ/E' ; IR, R)
747 sh			725 vw	
		603 w		
		491 m		
273 vw				
	252 m			
	207 m			
192 s				
	155 w			Lattice vibrations
145 vw, sh		139 w		
132 vs	128 w			
122 vw, sh				
		108 vw		
84 vw, sh				

s, Strong; m, medium; w, weak; v, very; sh, shoulder; br, broad.

3.3. Vibrational spectrum of $\text{Co}(\text{NO}_3)_2$

The corresponding FIR and Raman frequencies of **3** are given in Table 2 along with their proposed assignment. While the presented IR data of **1** are in fair agreement with the corresponding published IR frequencies [23,24], our IR values of **3** (Table 2) are in fair accordance with these in Ref. [25] but they disagree with those given in Ref. [24].

According to Ref. [15] $\text{Co}(\text{NO}_3)_2$ crystallizes in the trigonal space group $R\bar{3}$ (no. 148) and $Z=12$ ($Z^{\text{B}}=4$). As in $\text{Cd}(\text{NO}_3)_2$ and $\text{Pb}(\text{NO}_3)_2$ [26] the nitrate units in **3** are mainly ionic bonded. Therefore, the interpretation of the vibrational spectra of **1** and **3** might proceed from the NO_3^- anion with D_{3h} symmetry. Its vibrational analysis [27] does yield the following distribution of the fundamentals

$$\Gamma_{\text{vib}}(\text{NO}_3^-/D_{3h}) : A'_1(\text{R}) + A'_2(\text{IR}) + 2 E'(\text{R, IR}).$$

The pulsation ν_1 (A'_1) dominates the Raman spectrum of ionic nitrates whereas the asymmetrical stretching ν_3 (E') is the most intense in the IR spectra. The out-of-plane mode ν_2 (A'_2) is only IR active, but the combination $2\nu_2$ is often

found in Raman spectra of nitrates [28]. Finally, ν_4 (E') is the bending mode.

Comparing the ν_1 (A'_1) mode of the series of the alkali nitrates as well as that of AgNO_3 in solution, and in the crystalline and molten state, Bues [28] found the frequency range from 1035 cm^{-1} (solid AgNO_3) to 1086 cm^{-1} (solid LiNO_3), whereas the ν_1 mode of the “free” nitrate anion in solution is found at 1048 cm^{-1} . With the exception of AgNO_3 , the ν_1 nitrate-mode dependency on the alkali cations is explained by the packing density respective the needed volume of NO_3^- ions in the solids only.

ν_1 for $\text{Co}(\text{NO}_3)_2 \cdot 6\text{H}_2\text{O} \rightarrow [\text{Co}(\text{H}_2\text{O})_6]^{2+} (\text{NO}_3^-)_2$ with 1057 cm^{-1} it does fit very well with the existence of ionic NO_3^- units. In **3**, ν_1 is found at 1079 cm^{-1} which agrees well with that of LiNO_3 corresponding to comparable ionic radii of $\text{Li}^+_{(6)}$ with $\text{Co}^{2+}_{(6)}$. In AgNO_3 , an additional specific Ag^+ effect causes a decrease of the N–O binding force in NO_3^- and therewith its lower ν_1 [28].

The asymmetric NO_3^- stretching ν_3 (E') is strongest in IR and mostly weak/very weak in Raman spectra. For the “free” NO_3^- , it is found at 1380 cm^{-1} (1.7 M NaNO_3 so-

lution [28]). In the crystalline alkali nitrates, it is detected close to this value [28] too, and this IR band is mostly broad and also sometimes splitted. For **1**, ν_3 (E') is measured at 1384 (vs) and 1355 (vw) cm^{-1} . **3** exhibits two very strong IR bands at 1389 and 1356 cm^{-1} , respectively. A weak counterpart at 1392 cm^{-1} is found in the corresponding Raman spectrum. The before-mentioned splitting of the IR bands could be caused by a lowered NO_3^- symmetry in the crystal lattice (site symmetry or crystal field splitting?).

The out-of-plane ν_2 (A_2') for the “free” NO_3^- is found at 830 cm^{-1} , and also for solid NaNO_3 and KNO_3 nearby [28]. For **1** two IR bands at 829 (m) and 807 (w) cm^{-1} are recorded, whereas for **3** three (splitted) IR modes at 829 (s), 806 (m) and 799 (vw) cm^{-1} are detected (Table 2).

The bending mode ν_4 (E') of **3** is found at 750 (m-s) and 747 (sh) cm^{-1} in the Raman spectrum with a weak IR counterpart at 752 cm^{-1} . It is slightly enhanced compared to this one of the “free” NO_3^- at 720 cm^{-1} [28]. Surprisingly, for **1** no Raman bands, but only two very weak IR wings at 751 and 725 cm^{-1} are detected.

The remaining NO_3^- frequencies (cf. Table 2) might be caused by lowered NO_3^- symmetry in the crystal, and combinations, respectively. The very low frequency Raman and IR modes are ascribed to lattice vibrations.

Summarizing, in anhydrous $\text{Co}(\text{NO}_3)_2$ the nitrate units are mainly ionic bonded comparable to, e.g., $\text{Cd}(\text{NO}_3)_2$, $\text{Pb}(\text{NO}_3)_2$ [26] and to the alkaline-earth nitrates of calcium to barium [28]. The vibrational spectra of **3** do not fit to a pronounced covalent bonding as, e.g., by nitrate-grouping ($-\text{O}-\text{NO}_2$) in relation to the number and position of the expected normal modes of vibration.

4. Conclusion

The slow thermal decomposition (quasi-isothermal driving modus) of $\text{Co}(\text{NO}_3)_2 \cdot 6\text{H}_2\text{O}$ (**1**) proceeds in three stages via tetra- and di-hydrate to $\text{Co}(\text{NO}_3)_2$. Rapid heating of **1** causes the formation of a hydrate melt changing the system drastically by incoupled side reactions and evaporation of HNO_3 and other volatile species. This might be the main reason for the quite differing results and findings of the thermal $\text{Co}(\text{NO}_3)_2 \cdot 6\text{H}_2\text{O}$ decomposition and also for its non-reproducibility. An other error source of the mentioned decomposition is eventually the formation of cobalt(III)oxonitrate by the reaction of leaving water with dense packed sample material. For further cobalt(II)nitrate decomposition at higher temperatures, the atmosphere is important, whereas in N_2 Co_3O_4 and in H_2/N_2 metallic cobalt is formed.

Acknowledgements

The authors thank K. Bode and A. Strohschein for the careful recording of the vibrational spectra.

References

- [1] M.J. Tiernan, E.A. Fesenko, P.A. Barnes, G.M.B. Parkes, M. Ronane, *Thermochim. Acta* 379 (2001) 163.
- [2] M. Longhi, L. Formaro, *J. Mater. Chem.* 11 (2001) 1228.
- [3] T. Nissinen, M. Leskelä, M. Gasik, J. Lamminen, *Thermochim. Acta* 427 (2005) 155.
- [4] P. Arnoldy, J.A. Moulijn, *J. Catal.* 93 (1985) 38.
- [5] S. Narayanan, R.P. Unnikrishnan, *J. Chem. Soc., Faraday Trans.* 93 (1997) 2009.
- [6] M. Simionato, E.M. Assaf, *Mater. Res.* 6 (2003) 535.
- [7] G. Jacobs, J.A. Chaney, P.M. Patterson, T.K. Das, J.C. Maillot, B.H. Davis, *J. Synchrotron Rad.* 11 (2004) 414.
- [8] L. Markov, K. Petrov, V. Petkov, *Thermochim. Acta* 106 (1986) 283.
- [9] S.A.A. Mansour, *Mater. Chem. Phys.* 36 (1994) 317.
- [10] K.T. Wojciechowski, A. Malecki, *Thermochim. Acta* 331 (1999) 73.
- [11] B.V. L'vov, A.V. Novichikhin, *Spectrochim. Acta Part B* 50 (1995) 1427.
- [12] J.G. Jackson, R.W. Fonsa, J.A. Holcombe, *Spectrochim. Acta Part B* 50 (1995) 1449.
- [13] M.A.A. Elmasry, A. Gaber, E.M.H. Khater, *J. Therm. Anal.* 52 (1998) 489.
- [14] A. Malecki, R. Gajerski, S. Labus, B. Prochowska-Klisch, K.T. Wojciechowski, *J. Therm. Anal. Calorim.* 60 (2000) 17.
- [15] G.A. Tikhomirov, K.O. Znamenkov, I.V. Morozov, E. Kemnitz, S.I. Troyanov, *Z. Anorg. Allg. Chem.* 628 (2002) 269.
- [16] V. Kaiser, S. Ebinal, F. Menzel, E. Stumpp, *Z. Anorg. Allg. Chem.* 623 (1997) 449.
- [17] K. Dehnicke, J. Strähle, *Chem. Ber.* 47 (1964) 1502.
- [18] E. Stumpp, G. Nietfeld, K. Steinwede, K.-D. Wageringel, *Synth. Met.* 7 (1983) 143.
- [19] E. Stumpp, H. Griebel, C. Ehrhardt, *Mater. Sci. Forum* 91–93 (1992) 283.
- [20] T. Hatakeyama, Z. Liu, *Handbook of Thermal Analysis*, John Wiley & Sons, Chichester, New York, Weinheim, Brisbane, Singapore, Toronto, 1998, p. 64; A. Arii, T. Kanaya, A. Kishi, N. Fujii, *Netsu Sokutei* 21 (1994) 151.
- [21] B.V. L'vov, V.L. Ugolkov, *Thermochim. Acta* 424 (2004) 7.
- [22] B.V. L'vov, *Thermochim. Acta* 424 (2004) 183.
- [23] H. Volkman, *Handbuch der Infrarot-Spektroskopie*, Verlag Chemie, Weinheim/Bergstr., 1972, p. 219.
- [24] C.C. Addison, B.M. Gatehouse, *J. Chem. Soc.* (1960) 613.
- [25] FDM Electronic Handbook, Fiveash Data Management Inc. FDM FTIR Spectra of Minerals and Inorganic Compounds, Cobalt Nitrate?, vol. 106, 2001 (<http://www.fdm-spectra.com>).
- [26] A.F. Wells, *Structural Inorganic Chemistry*, fifth ed., Clarendon, Oxford, 1984, p. 823.
- [27] J. Weidlein, U. Müller, K. Dehnicke, *Schwingungsspektroskopie*, Thieme, Stuttgart, New York, 1982, pp. 107–108.
- [28] W. Bues, *Z. Phys. Chem., N.F.* 10 (1957) 1–23.